Cent. Eur. J. Biol. • 7(3) • 2012 • 531-541
DOI: 10.2478/s11535-012-0038-z

VERSITA

Central European Journal of **Biology**

Delayed fluorescence imaging of photosynthesis inhibitor and heavy metal induced stress in potato

Research Article

Jaka Razinger[1,*], Luka Drinovec[2], Maja Berden-Zrimec[3]

[1]*Agricultural Institute of Slovenia, 1000 Ljubljana, Slovenia*

[2]*Aerosol d.o.o., 1000 Ljubljana, Slovenia*

[3]*Institute of Physical Biology, 1000 Ljubljana, Slovenia*

Received 09 November 2011; Accepted 13 March 2012

Abstract: Early chemical-induced stress in *Solanum tuberosum* leaves was visualized using delayed fluorescence (DF) imaging. The ability to detect spatially heterogeneous responses of plant leaves exposed to several toxicants using delayed fluorescence was compared to prompt fluorescence (PF) imaging and the standard maximum fluorescence yield of PSII measurements (Fv/Fm). The toxicants used in the study were two photosynthesis inhibitors (herbicides), 100 μM methyl viologen (MV) and 140 μM diuron (DCMU), and two heavy metals, 100 μM cadmium and 100 μM copper. The exposure times were 5 and 72 h. Significant photosynthesis-inhibitor effects were already visualized after 5 h. In addition, a significant reduction in the DF/PF index was measured in DCMU- and MV-treated leaves after 5 h. In contrast, only DCMU-treated leaves exhibited a significant decrease in Fv/Fm after 5 h. All treatments resulted in a significant decrease in the DF/PF parameter after 72 h of exposure, when only MV and Cd treatment resulted in visible symptoms. Our study highlights the power of delayed fluorescence imaging. Abundant quantifiable spatial information was obtained with the instrumental setup. Delayed fluorescence imaging has been confirmed as a very responsive and useful technique for detecting stress induced by photosynthesis inhibitors or heavy metals.

Keywords: *Cadmium • Chlorophyll fluorescence • Copper • Diuron • EMCCD camera • Heavy metals • Herbicides • Paraquat • Photosynthesis inhibitors • Solanum tuberosum • Visualization*

© Versita Sp. z o.o.

Abbreviations

DCMU - 3-(3,4-dichlorophenyl)-1,1-dimethylurea, diuron
DF - delayed fluorescence
DMSO - dimethyl sulfoxide
EMCCD - electron-multiplying charge-coupled device
F_0 - minimal fluorescence from dark-adapted leaf
Fm - maximum fluorescence from dark-adapted leaf
Fv - variable fluorescence measured in dark-adapted plant, $Fv=Fm-F_0$
Fv / Fm - maximum fluorescence yield of PSII, $Fv/Fm=(Fm-F_0)/Fm$
LED - light-emitting diode
MV - 1,1′-Dimethyl-4,4′-bipyridinium dichloride, methyl viologen (syn. paraquat)
PAM - pulse amplitude modulation
PAR - photosynthetically active radiation
PF - prompt fluorescence

1. Introduction

The introduction of non-invasive optical techniques to biological research has significantly decreased errors caused by sample manipulation and subjective interpretation of complex findings. Imaging has additionally improved analysis of higher plants because

* *E-mail: jaka.razinger@kis.si*

the molecular and physiological processes that alter the yield of chlorophyll fluorescence can vary substantially over the leaf surface [1]. Because of the spatial heterogeneity in leaf response to infection, imaging and its analysis are extremely important for reasonable determination of various stresses [2,3]. This is especially crucial for early detection of infection, when fast action prevents the spread of disease.

Although there are numerous studies of higher plants using prompt fluorescence imaging [1,4], only a few publications deal with delayed fluorescence imaging. Bennoun and Beal [5] successfully screened algal mutant colonies with an altered thylakoid electrochemical gradient using delayed fluorescence digital imaging. Flor-Henry *et al*. [6] imaged delayed fluorescence from a leaf surface; however, their research was preferentially aimed toward ultra-weak luminescence from damaged leaves. Early works on DF visualization dealt with damage to the photosynthetic system caused by viruses, insects, temperature extremes, ultraviolet radiation, or herbicides [7], whereas Ellenson and Amundson [8] investigated the spatial distribution and temporal development of plant stress using DF visualization.

There are several differences between delayed and prompt fluorescence. Delayed fluorescence (DF) is a long-lived (from milliseconds to seconds) low-level photon emission from plant tissue after a short illumination pulse [9]. During the illumination, charge pairs are generated in photosystem II (PSII), with positive charges located on the oxygen-evolving complex and negative charges on the quinone acceptors (Q_A and Q_B). The slow components of DF originate in back reactions between the S_2 and S_3 states of the oxygen-evolving complex and quinones Q_A and Q_B [10]. The half-times of these reactions in isolated chloroplasts are 1 to 2 s for $Q_A^-S_{2/3}$ and approximately 25 s for $Q_B^-S_{2/3}$ [11]. Prompt fluorescence (PF), on the other hand, originates in the radiative de-excitation of excited chlorophyll molecules before charge separation emitted in the nanosecond time range. DF is affected by chemical and physical parameters, such as various chemicals and metals [12-16], temperature [17], or nutrient status [18]. The intensity of delayed fluorescence has been reported to be a measure of photosynthetic activity [19]. DF decay kinetics depend on the rates of back reactions in the electron backflow in the photosynthesis electron transport chain [12,20]. These differences in the physiology of the DF and PF result in some advantages of DF-based parameters over PF: the DF signal can change by a factor of 10 or more, whereas the PF parameters would change by a factor of about three during certain fluorescence measurements [21].

To see the effect on the photosynthetic apparatus of *Solanum tuberosum* leaves, we applied two photosynthesis inhibitors: methyl viologen (MV, also known as paraquat) and diuron (DCMU), as well as two heavy metals: cadmium and copper. DCMU affects the acceptor side of PSII, where it competes with plastoquinone and plastoquinol for the Q_B binding site, preventing electron flow between photosystem II (PSII) and the plastoquinone pool [22]. This inhibition of the slow components of DF results in faster decay of DF [11]. MV acts as an electron acceptor from PSI and transfers the electrons to molecular oxygen-producing reactive oxygen species (ROS) [23]. It is believed that copper binds to PSII [24] and inhibits protein synthesis in chloroplasts as well as the reactions of the Calvin cycle [25,26]. As a transition metal, it can also participate in Fenton chemistry, producing ROS, which can damage biological macromolecules [27]. Cadmium interferes with the oxygen-evolving complex in PSII, the plastoquinone pool, and ribulose-1,5-bisphosphate carboxylase oxygenase (RubisCo) synthesis [28,29]. It is not a redox active-transition metal, but can indirectly expedite ROS production by substituting an essential micronutrient (e.g., disturbing Fe homeostasis; [30]) or binding non-specifically to thiol groups, thereby disturbing various metabolic processes [31].

Our aims were (a) to assess whether delayed fluorescence can be accurately visualized to enable quantification, and (b) to determine whether delayed fluorescence imaging makes it possible to see a spatially heterogeneous response of plant leaves to stress induced by either photosynthesis inhibitors or heavy metals. In addition, a quotient of DF and PF images was calculated to provide a normalized photosynthetic stress parameter.

2. Experimental Procedures

2.1 Plant material and exposure to the chemicals tested

The experiments were performed on excised leaves of *Solanum tuberosum* L. var. Sante [32]. The plants were grown from tissue culture. They were kept in a growth chamber at 21±1°C, 70±2% relative humidity, under cool white fluorescent light (160 μmol m^{-2} s^{-1} photosynthetically active radiation, PAR) with a light:dark cycle of 18:6 h. When the plants were 6 weeks old, fully matured leaves from the middle-top of the canopy were cut and their petioles inserted into 4 ml cuvettes filled with previously prepared dilutions of the chemicals tested in half-strength Steinberg growth medium [33]. The cuvettes with the leaves were then sealed with parafilm to minimize evaporation and put into the growth chamber. After 5 or 72 h the leaves were removed from the test cuvettes and the leaf stalks washed with distilled

water, put into fresh half-strength Steinberg growth medium, and placed in darkness.

2.2 Chemicals

All chemicals were purchased from Sigma (distributor: Mikro + Polo d.o.o., Maribor, Slovenia), unless stated otherwise. They were of the highest commercially available grade possible, 99% or more pure. The following stock solutions were prepared: 7 mM DCMU (3-(3,4-dichlorophenyl)-1,1-dimethylurea; also known as diuron) in dimethyl sulfoxide (DMSO; Kemika, Zagreb, Croatia), 10 mM methyl viologen dichloride (MV; 1,1′-Dimethyl-4,4′-bipyridinium dichloride; also known as paraquat), 10 mM $CdCl_2$, and 10 mM $CuSO_4$ in double-distilled water. Working dilutions were prepared in half-strength Steinberg growth medium [33] to provide adequate nutrients for the leaves. The final concentrations of MV, $CdCl_2$, or $CuSO_4$ were 100 µM and 140 µM for DCMU. For the control, we used half-strength Steinberg growth medium alone. The concentration of DMSO in the final dilution for DCMU treatment was 2%, which did not affect the *S. tuberosum* leaves.

2.3 Visualization measuring setup

Fluorescence and delayed fluorescence imaging was performed in a dark measuring chamber. For sample illumination, a 435 nm light-emitting diode (LED) module (LED435-66-60, Roithner Lasertechnik, Vienna, Austria) with a band-pass filter 447±30 nm (Semrock FF01-447/60-25, New York, NY, USA) was used connected to an illumination ring to ensure optimal and homogenous sample illumination. The LED module was powered by two different current generators to obtain 100 µmol m^{-2} s^{-1} PAR and 0.13 µmol m^{-2} s^{-1} PAR for the HIGH/LOW light options. Images were captured by an EMCCD camera (L3Vision CCD65, e2v Technologies, Chelmsford, UK) Peltier cooled to −5°C, equipped with a 12.0 mm focal-length compact VIS-NIR Lens (Schneider, Edmund Optics, Barrington, NJ, USA) and a 635 nm long-pass filter (Semrock FF01-635/LP-25, New York, NY, USA). Frame-grabber (MovieBox Deluxe, Pinnacle Systems, Mountain View, CA, USA) and video-editing software (Pinnacle Studio Plus V9.42, Pinnacle Systems, Mountain View, CA, USA) were used to obtain 24 frame-per-second videos. A multifunction data-acquisition device (DAQPad 6015, National Instruments, Austin, TX, USA) was used for LED and shutter control (Figure 1).

2.4 Data acquisition

Before measurement, each leaf was transferred to the dark measuring chamber and covered with museum-quality non-glare glass (ClearColor Plus UV, NielsenBainbridge, Germany) to smooth the surface of the leaf and ensure uniform lighting conditions. Prior to the measurement, leaves were dark-adapted for 10 min. The EMCCD camera gain was set on maximum (fluorescence signal amplified 330-fold). For prompt fluorescence measurement, samples were illuminated with low-power illumination (0.13 µmol m^{-2} s^{-1} PAR) for 1 s while the camera was simultaneously recording the

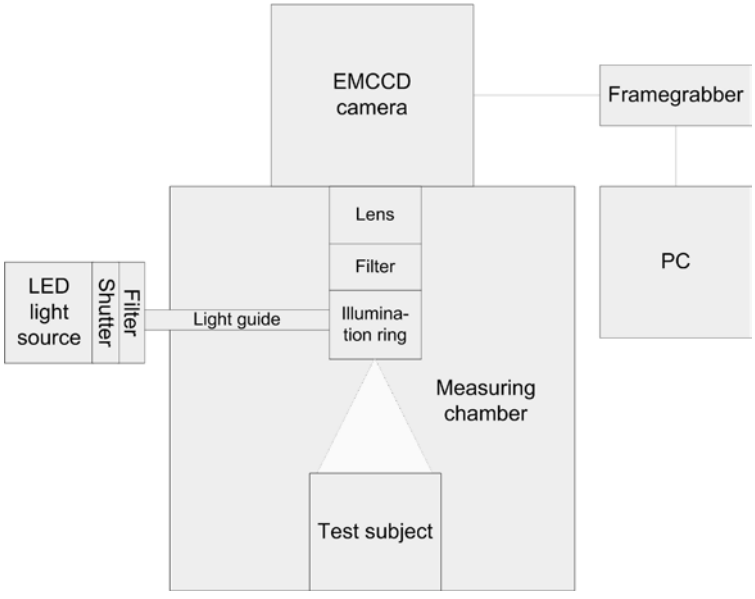

Figure 1. Experimental setup. The excitation light was produced by a LED light source equipped with a shutter and a filter. The sample was homogenously illuminated through an illumination ring connected to the LED light source by an optical light guide. The emitted light was detected by a cooled EMCCD camera equipped with a filter and a fast macro lens. Data were captured by a frame grabber and sent to a PC for further analysis. Note: The scheme is not drawn to scale. The actual distance between the object (leaf) and the objective was approximately 24 mm.

data. For DF measurement, samples were illuminated for 1.5 s with high-power illumination (100 µmol m^{-2} s^{-1} PAR), then the light was switched off and the shutter closed to avoid detection of any scattered light. The reason to use a shutter is the weak light emission we observed from blue LEDs lasting for about 1 second after being switched off. Without the shutter, prompt fluorescence would be induced, which would interfere with the delayed fluorescence measurements. DF measurement started immediately after the shutter was closed and lasted for 20 seconds.

2.5 Determination of illumination homogeneity

The illumination conditions were examined before each experiment. A piece of uniformly white paper was put on the sample plate of the measuring chamber. LED illumination in the HIGH setting was used because at this illumination intensity sufficient excitation light reflected by the paper passed the emission filter to be detected by the camera. Under high-yield LED illumination, 1 s video clips were captured; 10 frames were extracted and averaged using custom-made software. Noise was subtracted from the averaged image using ImageJ software, versions 1.35s and 1.43u (Wayne Rasband, National Institute of Health, USA). Then the image was examined in ImageJ. The heterogeneity of images in the central region of the field was less than 5% (radius of 20 mm). Across the entire field of observation, the heterogeneity of images was less than 10% (radius of 60 mm). In the experimental setup the illumination ring was 17 mm from the leaves. The objective lens was approximately 24 mm from the leaves.

2.6 PF images

One-second video clips were captured under low-power illumination as described above. Ten frames were extracted and averaged using custom-made software. Background subtraction and all subsequent image manipulation were performed in ImageJ. The resulting images were divided by the image of illumination homogeneity in order to normalize the fluorescence signal to the illumination intensity. To increase the contrast, the image histogram was stretched by setting the maximum pixel intensity to 3.

2.7 DF images

All frames were extracted from 20 s DF video clips. Frames 10 to 430 were averaged to obtain DF images. The background was subtracted from the original DF images and contrast enhanced in ImageJ.

2.8 PF, DF, and DF/PF intensity

Due to differential intoxication in the case of DCMU and MV, the images from these two treatments were quantified differently in 5 or 72 h experiments: in the 5 h experiments two regions in the case of DCMU (the midrib and the leaf edge) and three regions in the case of MV (the midrib, lamina, and leaf edge) were measured by placing a circular measuring area with a radius of 20 pixels over the areas of interest. In control, Cd and Cu treatments in 5 h experiments, and all treatments in 72 h experiments, only the central (midrib) regions of the leaves were analyzed. Here a circular measuring area with a radius of 45 pixels was used. Measurements over the central vein were avoided when possible. In addition, the circular measuring area was much larger than the central vein area. The mean, standard deviation, and distribution of the pixel values were analyzed. The coordinates of the intensity measurements and the histograms were saved to enable traceability of the data-acquisition process. The mean values were used in the subsequent statistical analysis.

2.9 Fv/Fm measurements

In vivo chlorophyll *a* fluorescence was measured using a non-imaging pulse amplified modulation (PAM) fluorometer (OS5-FL, Opti-Sciences, Hudson, NH, USA). Minimal fluorescence (F_0) was obtained after 10 minutes of dark adaptation using a dark clip. The clip was positioned over the central portion of the leaf lamina. Maximal fluorescence (Fm) was determined after exposure to a 0.8 s saturating pulse of white light (about 8,000 µmol photons m^{-2} s^{-1}). From the measured fluorescence data, the maximum quantum yield of PSII photochemistry $Fv/Fm=(Fm-F_0)/Fm$ was calculated [34]

2.10 DF kinetics

The data for DF kinetics analyses were obtained as in PF, DF, and DF/PF intensity analysis. Thus each frame from DF video clips was analyzed. Our measuring setup enabled us to obtain the DF signal in a time range of 0.42 to 20 s after the sample illumination with a time resolution of 24 frames/s. Delayed fluorescence was fitted to the hyperbolic curve $I=I_0(t+t_0)^{-m}+I_b$, where I_0, t_0, m, and I_b are the fitting parameters. I_b was introduced to compensate for background noise. Parameter m represents the slope of the decay curve with higher values corresponding to faster decay. Data were fitted using the non-linear fitting algorithm of the Microcal Origin software (OriginLab, Northampton, MA, USA). In all cases fit was very good, with R^2 between 0.95 and 0.9998.

2.11 Statistical analysis

All experiments were repeated independently three times in triplicate (three leaves per treatment). Subsequently, the data from different experiments were pooled (n=9).

All data were computer analyzed using MS Excel 2003 and GraphPad Prism 5 for Windows. One-way analysis of variance and Dunnett's Multiple Comparison Test were performed on all data. The difference between exposed and control plants was considered significant at P levels lower than 0.05 (P<0.05); significance is denoted in the figures by an asterisk (*). The statistical significance of treatments in 5 or 72 h experiments was tested against 5 or 75 h controls, respectively.

3. Results

3.1 Visible symptoms

The excised *Solanum* leaves treated with either photosynthesis inhibitors or heavy metals did not exhibit any symptoms visible to the naked eye after 5 h exposure to the toxicants (not shown). After 72 h of exposure, however, severe chlorosis, necrosis, leaf wrinkling, and drying were observed in MV-treated leaves. The Cd-treated leaves were somewhat chlorotic, with about 10% of the leaves' laminas necrotic. The Cu, DCMU, or control treatment did not result in any visible toxicity symptoms after 72 h of exposure (Figure 2).

3.2 Prompt and delayed chlorophyll fluorescence images

Figure 3 represents a composite of all images obtained from a typical 5 h experiment. The control as well as Cd- and Cu-treated leaves exhibited a uniform response across the leaf lamina, without any obvious stress symptoms; similar values of PF, DF, and DF/PF intensity were measured in these treatments. In DCMU-treated leaves, we measured higher PF and lower DF intensity in the central part of the leaves and in the area surrounding the main leaf veins. DF/PF intensity was lower in the central part of the DCMU-treated leaves as compared to unaffected leaf edges. MV treatment had no effect on PF intensity, but considerably reduced DF intensity around the midrib and somewhat less in the area surrounding the leaf veins. Similar results were observed and measured in the DF/PF images.

3.3 Analysis of PF images

Significant increases in prompt fluorescence were measured in DCMU-intoxicated areas of leaves during the 5 and 72 h experiments (Figure 4). 100 μM

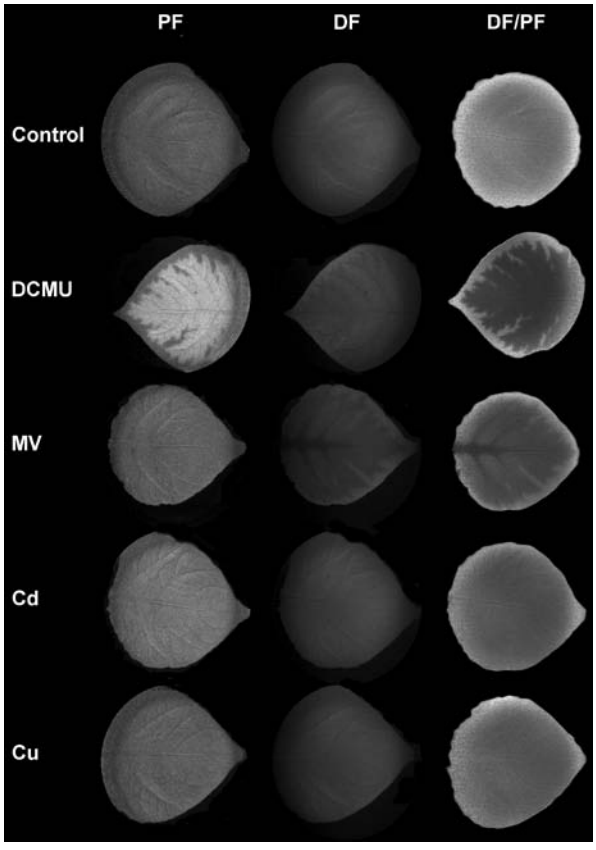

Figure 3. Raw chlorophyll fluorescence images from a typical 5 h experiment. *DCMU* = diuron 140 μM; *MV* = methyl viologen (paraquat) 100 μM; *Cd* = $CdCl_2$ 100 μM; *Cu* = $CuSO_4$ 100 μM; *PF* = prompt fluorescence; *DF* = delayed fluorescence; *DF/PF* = normalized index.

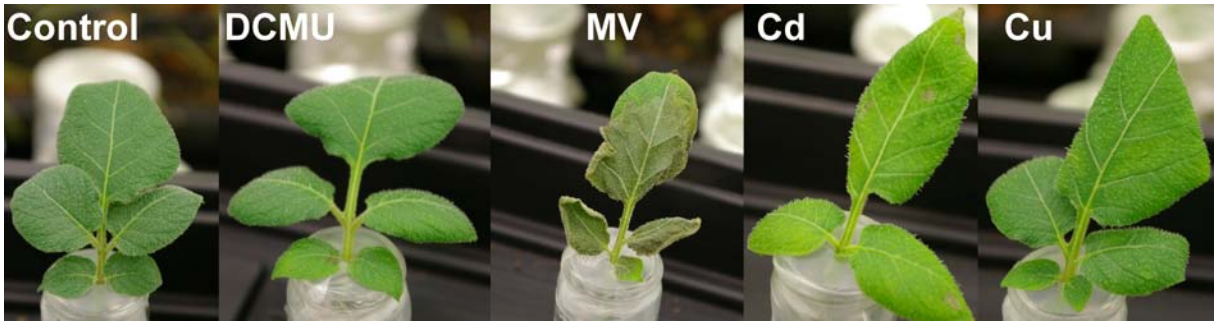

Figure 2. A digital composite image of photosynthesis inhibitors and heavy metal toxicity symptoms in the plant leaves after 72-h exposure. *DCMU* = diuron 140 μM; *MV* = methyl viologen (paraquat) 100 μM; *Cd* = $CdCl_2$ 100 μM; *Cu* = $CuSO_4$ 100 μM.

MV decreased whereas 100 µM $CuSO_4$ and 100 µM $CdCl_2$ increased PF during 72 h experiments; however, these changes were not significant.

3.4 Analysis of DF images

Delayed fluorescence significantly decreased in DCMU and MV-intoxicated areas of leaves during 5 and 72 h experiments. On the other hand, 100 µM $CuSO_4$ and 100 µM $CdCl_2$ exhibited time-dependent effects on DF: copper significantly decreased DF during short-term exposure (5 h), whereas cadmium significantly decreased DF during 72 h experiments (Figure 5).

3.5 Analysis of DF / PF images

DF/PF image analysis revealed a significant decrease in the midrib area of leaves in both the 140 µM DCMU and 100 µM MV-treated groups, as well as most of the lamina in the 100 MV-treated groupin 5 h experiments. During

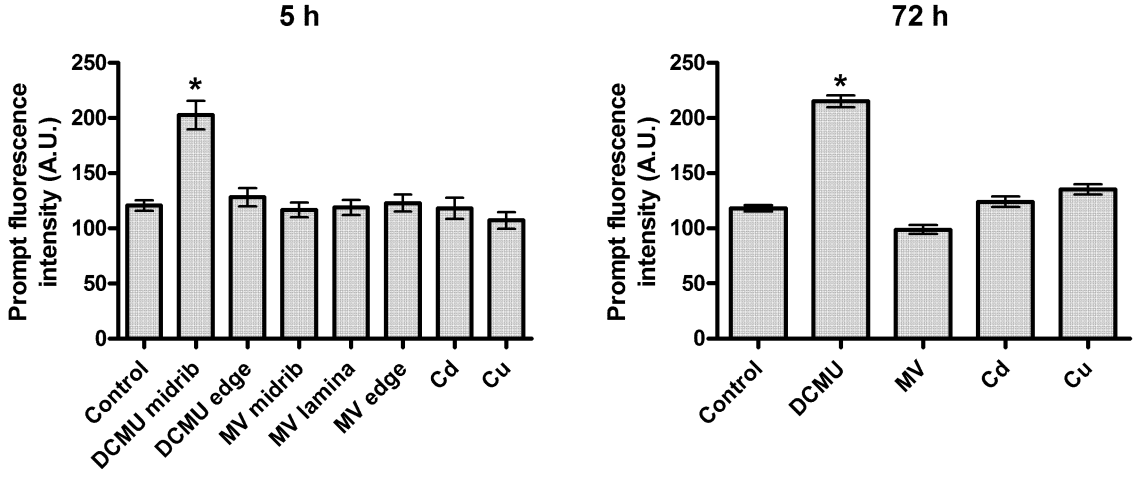

Figure 4. Prompt fluorescence (PF) image analysis from 5 and 72 h experiments. The dark-adapted potato leaves were illuminated with a weak actinic light while prompt fluorescence image data were captured. The data shown are mean values ± standard error of three independent experiments performed in triplicate (n=9). *DCMU* = diuron 140 µM; *MV* = methyl viologen (paraquat) 100 µM; *Cd* = $CdCl_2$ 100 µM; *Cu* = $CuSO_4$ 100 µM. *A.U.* = arbitrary unit. An asterisk (*) denotes a significant difference between exposed and control plants of 5 or 72 h experiments (P<0.05).

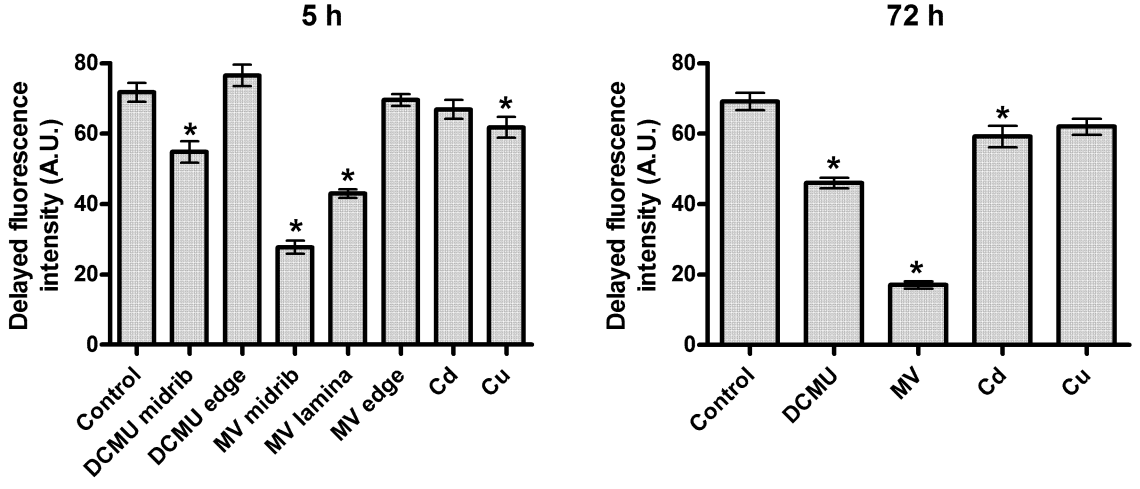

Figure 5. Delayed fluorescence (DF) image analysis from 5 and 72 h experiments. The dark-adapted potato leaves were illuminated with a 100 µmol $m^{-2}s^{-1}$ PAR light pulse before DF images were captured. Data shown are mean values ± standard error of three independent experiments performed in triplicate (n=9). *DCMU* = diuron 140 µM; *MV* = methyl viologen (paraquat) 100 µM; *Cd* = $CdCl_2$ 100 µM; *Cu* = $CuSO_4$ 100 µM; *A.U.* = arbitrary unit. An asterisk (*) denotes a significant difference between exposed and control plants of 5 or 72 h experiments (P<0.05).

72 h experiments we measured a significant decrease in the DF/PF index in all treatments. The DF/PF index in control leaves growing for 72 h in the growth chambers was not significantly lower than the DF/PF index in control leaves from 5 h experiments (0.191±0.014 at 5 h and 0.174±0.004 at 72 h; P=0.195; Figure 6).

3.6 Measurements of maximum fluorescence yield of PSII (Fv/Fm)

During 5 h experiments only 140 µM DCMU caused significant reductions in maximum quantum yield of PSII photochemistry. During 72 h experiments both photosynthesis inhibitors (140 µM DCMU and 100 µM MV) as well as 100 µM $CdCl_2$ caused significant reductions in maximum quantum yield of PSII photochemistry (Figure 7).

3.7 Delayed fluorescence decay kinetics

In addition to spatial differences in DF intensity (Figure 3), delayed fluorescence decay kinetics fitted to the hyperbolic curve $I=I_0(t+t_0)^{-m}+I_b$ differed between treatments (Figure 8). The most informative was the parameter m, which corresponds to the slope of the decay. DCMU caused a significant increase of

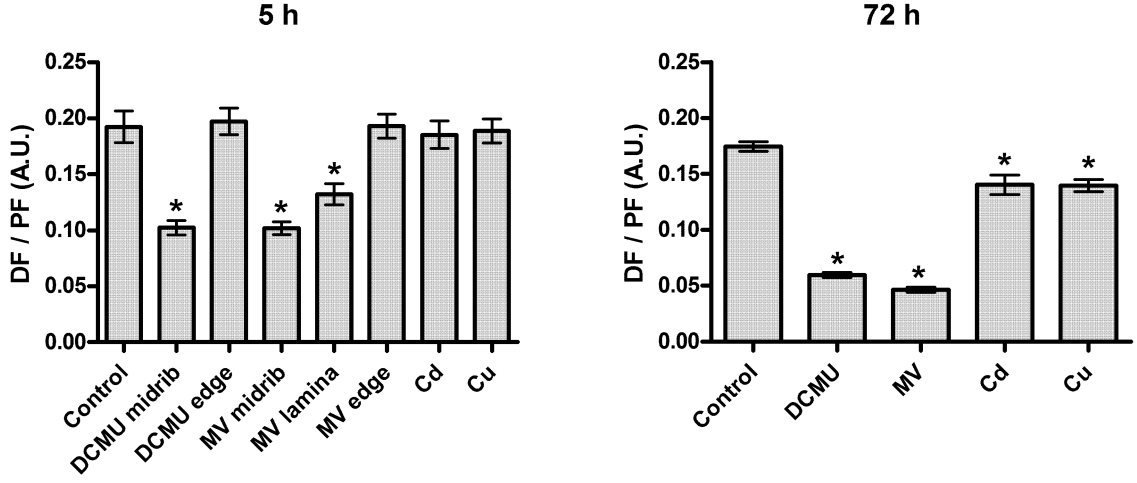

Figure 6. Analysis of the quotient of delayed fluorescence (DF) and prompt fluorescence (PF) images from 5 and 72 h experiments. Data shown are mean values ± standard error of three independent experiments performed in triplicate (n=9). *DCMU* = diuron 140 µM; *MV* = methyl viologen (paraquat) 100 µM; *Cd* = $CdCl_2$ 100 µM; *Cu* = $CuSO_4$ 100 µM; *A.U.* = arbitrary units. An asterisk (*) denotes a significant difference between exposed and control plants of 5 or 72 h experiments (P<0.05).

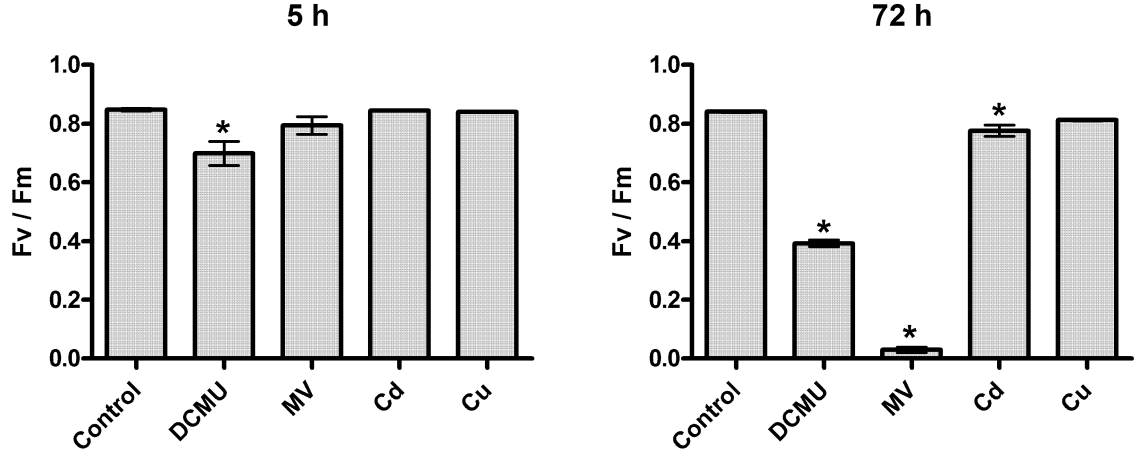

Figure 7. Maximum quantum yield of PSII photochemistry (Fv/Fm) measured after 5 and 72 h of exposure. Data shown are mean values ± standard error of three independent experiments performed in triplicate (n=9). Measurements were performed on the central areas of leaves in all treatments in 5 and 72 h experiments. *DCMU* = diuron 140 µM; *MV* = methyl viologen (paraquat) 100 µM; *Cd* = $CdCl_2$ 100 µM; *Cu* = $CuSO_4$ 100 µM; *A.U.* = arbitrary unit. An asterisk (*) denotes a significant difference between exposed and control plants of 5 or 72 h experiments (P<0.05).

parameter *m* in the midrib region and an insignificant increase in the less-intoxicated leaf edge after 5 h of exposure. MV caused a significant decrease of *m*, which was most pronounced in the midrib area. There was also a small but significant increase of *m* in the case of copper exposure. At the 72 h time point only DCMU caused a significant change in parameter *m*.

3.8 Heterogeneity of the fluorescence signal

In the 5 h experiments, the intoxication in the case of DCMU and MV varied across the leaf lamina, with the midrib being the most affected and the leaf edge the least. After 72 h of exposure, however, the entire leaf laminas were uniformly intoxicated in these two as well as in all other treatments. Figure 9 represents how the two-dimensional image data were reduced and analyzed in the 5 h experiments.

4. Discussion

Our experimental setup, utilizing a cooled electron-multiplying CCD camera, enabled us to successfully visualize delayed and prompt fluorescence of *S. tuberosum* leaves. DF and PF images showed the heterogeneous influence of photosynthesis inhibitors and metals on the surface of leaves. The most pronounced effect of MV was observed in the midrib area, and DCMU in the central part of lamina, whereas metal exposure resulted in a very even response across the entire leaf area (Figures 3, 9).

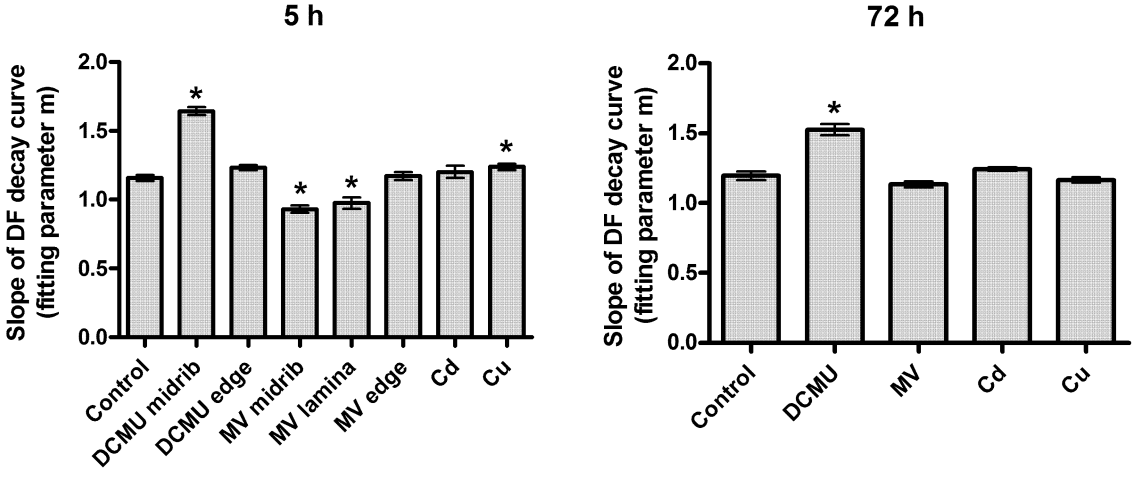

Figure 8. Slope of DF decay kinetics represented as parameter *m* of the hyperbolic curve $I=I_0(t+t_0)^{-m}+I_b$, to which the data were fitted. The DF kinetics were measured on the same regions of the leaves as in the PF, DF, and DF/PF analyses. The data shown are mean values ± standard error of three independent experiments performed in triplicate ($n=9$). *DCMU* = diuron 140 μM; *MV* = methyl viologen (paraquat) 100 μM; *Cd* = $CdCl_2$ 100 μM; Cu = $CuSO_4$ 100 μM; *A.U.* = arbitrary unit. An asterisk (*) denotes a significant difference between the exposed and control plants ($P<0.05$).

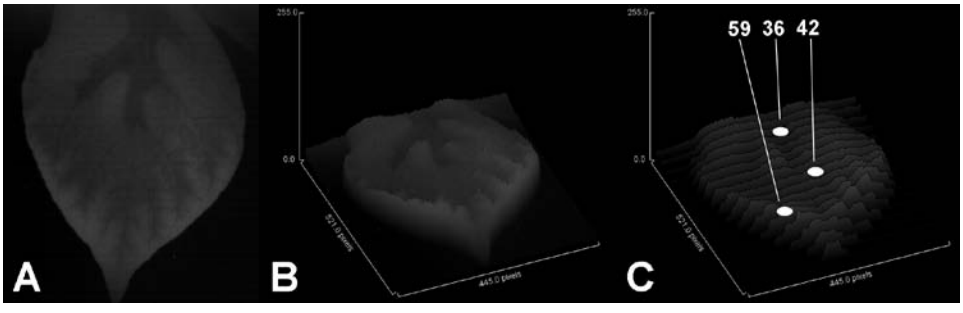

Figure 9. A representation of the heterogeneous distribution of the DF signal obtained from a potato leaf intoxicated for 5 hours with 100 μM MV. (A) spatial heterogeneity of the original DF signal; (B) transformation of DF data onto a three-dimensional surface; (C) pixel intensity profiles across the entire leaf surface. In (C) the places of data acquisition as well as the DF intensity values for this specific leaf are marked.

Delayed fluorescence responded to all applied chemicals already after 5 h exposure, although there was no visible damage at that time. DCMU strongly interferes with electron transport by blocking a Q_B binding site on PSII. As a consequence, DF yielding back-reactions between the oxygen-evolving complex and Q_B are inhibited. DCMU begins to cause a decrease of DF approximately 2 s after illumination [17]. With our experimental setup, we managed to measure this expected decrease of DF using long acquisition intervals (20 s). Reductions in DF after 5 h were most prominent in the case of MV exposure. MV resulted in a gradient of DF that increased with increasing distance from the central vein (Figures 3, 5). Different DF decay kinetics were observed in leaves treated with different chemicals (Figure 8). In addition, different DF decay kinetics were observed in regions of leaves with varying MV or DCMU intoxication (Figure 8). MV influences electron transport as a strong electron sink at the acceptor side of PSI [23], thus causing oxidation of the plastoquinone pool. A consequence is the lower rate of reversed electron flow to the PSII, manifested in lower DF intensity. Decreases in DF after 5 h of MV exposure cannot be attributed solely to oxidative damage to the PSII [35] because Fv/Fm was only slightly reduced at the same time (Figure 7). Part of the DF reduction could also be attributed to the oxidation of PSI caused by MV. However, this effect is limited to only 1 to 2% of the DF that is emitted from PSI [36].

Prompt fluorescence imaging did not show significant effects of MV, cadmium, or copper. The increase in PF after 72 h exposure to Cd and Cu showed some PSII damage in the exposed leaves (Figure 4). The increase in PF intensity by DCMU exposure could be attributed to the fact that even our lowest possible illumination intensity (0.13 $\mu mol\, m^{-2} s^{-1}$ PAR) was enough to cause closure of the reaction centers [24]. The illumination intensity of the light utilized for PF imaging was low enough to obtain the minimum fluorescence (F_0) in all other cases. A real F_0 value in PF-imaging experiments in DCMU exposure could be obtained by the pulse-modulation imaging method [37]. This was not possible with our experimental setup.

Maximum quantum yield of PSII photochemistry (Fv/Fm) measurement, obtained using a commercial PAM fluorometer at 5 h, showed a significant decrease only in the case of DCMU, which could again be attributed to inaccurate F_0 measurement. After 72 h, Fv/Fm of DCMU-exposed leaves was reduced to less than half that of the controls in the case of DCMU and almost to zero in the case of MV showing strong PSII damage. Fv/Fm was also reduced by 72 h exposure to cadmium (Figure 7). These measurements coincide well with visual observations at 72 h, when only MV and Cd treatment resulted in symptoms visible to the unaided eye.

The DF/PF index was introduced as a normalized parameter to test the fitness of the photosynthetic apparatus. A similar parameter has been introduced before [18], in which F_0 was used instead of PF. DF/PF was selected as a promising stress parameter because PF increases with the number of non-active PSII reaction centers, whereas DF increases with the concentration of active PSII centers [12]. When the number of active PSII reaction centers is reduced, DF/PF values should decrease. In *Dunaliella tertiolecta*, DF/PF was more sensitive to nitrogen deprivation than Fv/Fm [18]. In this study, DF/PF was shown to be the best phenomenological stress parameter: after only 5 h of exposure to DCMU and MV, a 50% reduction (compared to the control) was measured in the most intoxicated areas of leaves (Figure 6). The effect of these chemicals is even more evident after 72 h. In addition, the effects of copper and cadmium significantly decreased the value of DF/PF at this time point, which is quite expected due to the wide spectrum of toxic action of the selected metals on the photosynthetic apparatus [29] and various metabolic processes [27,30].

DF decay kinetics were steeper (higher *m* values) in the case of DCMU, which is in accordance with published data [11]. MV caused transient reduction of parameter *m*, which diminished after 72 h. At this time point, general toxicity symptoms surpassed the direct inhibitory action of MV, as shown by a strong reduction of DF intensity. In copper-exposed leaves we observed a small but significant increase of *m* at 5 h (Figure 8). Despite the sensitivity of parameter *m* to the chemicals tested, it cannot be used as a general stress marker because of its specific responses to different chemicals.

We have shown that delayed fluorescence imaging allowed us to detect stress symptoms considerably sooner than they can be observed visually. In this way it competes with the more common prompt fluorescence imaging, which has already proved its applicability in research on photosynthesis, detection of fungal infection, discrimination of heterogeneous populations of algal cells within intact biofilms, and detection of herbicide effects [1,4,38]. Although the basic mechanism of DF is well understood, straightforward interpretation of the influence that different stressors have on DF can

be risky due to the complex interplay of the processes that influence DF kinetics and intensity. However, the robustness and sensitivity of DF as a measure of photosynthetic activity has its advantages in studies of plant physiology and toxicology [12,13,15,39,40].

5. Conclusions

Our study highlights the power of delayed fluorescence imaging for detection of early stress and damage to the photosynthetic apparatus. In addition to the abundant spatial and temporal information obtained with our instrumental setup, it is evident that delayed fluorescence imaging is more responsive compared to prompt fluorescence parameters. The study demonstrates that already after 5 h, when toxicity symptoms are indiscernible to the observer, significant effects of two common photosynthesis inhibitors (herbicides) can be visualized. The DF/PF index was shown to be a sensitive and robust index that allowed us to normalize delayed fluorescence imaging data. Thus we were able to quantify photosynthesis damage by herbicides as well as heavy metals and compare this damage in different leaves.

Acknowledgements

This research was partly financed by the Slovenian Research Agency, grants 3311-04-831833, J1-6473, L4-6222, V4-0106, and P1-0212. We are grateful to Maja Kovač from the Slovenian National Institute of Biology for providing the *S. tuberosum* plants.

References

[1] Nedbal L., Whitmarsh J., Chlorophyll fluorescence imaging in leaves and fruits, In: Papageorgiou G.C., Govinjee (Eds.), Chlorophyll a fluorescence: A signature of photosynthesis, Springer, Dordrecht, 2004

[2] Chaerle L., Van Der Straeten D., Seeing is believing: imaging techniques to monitor plant health, Biochim Biophys Acta, 2001, 1519, 153–166

[3] Baker N.R., Rosenqvist E., Applications of chlorophyll fluorescence can improve crop production strategies: an examination of future possibilities, J Exp Bot., 2004, 55, 1607–1621

[4] Oxborough K., Imaging of chlorophyll a fluorescence: theoretical and practical aspects of an emerging technique for the monitoring of photosynthetic performance, J Exp Bot, 2004, 55, 1195–1205

[5] Bennoun P., Beal D., Screening algal mutant colonies with altered thylakoid electrochemical gradient through fluorescence and delayed luminescence digital imaging, Photosynth Res, 1997, 51, 161–165

[6] Flor-Henry M., McCabe T.C., de Bruxelles G.L., Roberts M.R., Use of a highly sensitive two-dimensional luminescence imaging system to monitor endogenous bioluminescence in plant leaves, BMC Plant Biol, 2004, 4, 19

[7] Björn L.O., Forsberg A.S., Imaging by Delayed Light Emission (Phytoluminography) as a Method for Detecting Damage to the Photosynthetic System, Physiol Plant, 1979, 47, 215–222

[8] Ellenson J.L., Amundson R.G., Delayed light imaging for the early detection of plant stress, Science, 1982, 215, 1104-1106

[9] Strehler B.L., Arnold W., Light production by green plants, J Gen Physiol, 1951, 34, 809–820

[10] Joliot P., Joliot A., Bouges B., Barbieri G., Studies of system-II photocenters by comparative measurements of luminescence, fluorescence, and oxygen emission, Photochem Photobiol, 1971, 14, 287–305

[11] Rutherford A.W., Inoue Y., Oscillation of delayed luminescence from PSII recombination of S2QB- and S3QB-, FEBS Lett, 1984, 165, 163–170

[12] Joliot P., Joliot A., Dependence of delayed luminescence upon adenosine triphosphatase activity in Chlorella, Plant Physiol, 1980, 65, 691–696

[13] Drinovec L., Drobne D., Jerman I., Zrimec A., Delayed fluorescence of Lemna minor: a biomarker of the effects of copper, cadmium, and zinc, Bull Environ Contam Toxicol, 2004, 72, 896–902

[14] Katsumata M., Koike T., Nishikawa M., Kazumura K., Tsuchiya H., Rapid ecotoxicological bioassay using delayed fluorescence in the green alga Pseudokirchneriella subcapitata, Water Res, 2006, 40, 3393–3400

[15] Berden-Zrimec M., Drinovec L., Zrimec A., Tisler T., Delayed fluorescence in algal growth inhibition tests, Cent. Eur. J. Biol., 2007, 2, 169–181

[16] Wang C., Xing D., Chen Q., A novel method for measuring photosynthesis using delayed fluorescence of chloroplast, Biosens Bioelectron, 2004, 20, 454–459

[17] Zrimec A., Drinovec L., Berden-Zrimec M., Influence of chemical and physical factors on long-term

delayed fluorescence in Dunaliella tertiolecta, Electromagn Biol Med, 2005, 24, 309–318

[18] Berden-Zrimec M., Drinovec L., Molinari I., Zrimec A., Fonda S., Monti M., Delayed fluorescence as a measure of nutrient limitation in Dunaliella tertiolecta, J Photochem Photobiol B-Biol, 2008, 92, 13–18

[19] Schneckenburger H., Schmidt W., Time-resolved chlorophyll fluorescence of spruce needles after different light exposure, J Plant Physiol, 1996, 148, 593–598

[20] Avron M., Schreiber U., Properties of ATP induced chlorophyll luminescence in chloroplasts. Biochim Biophys Acta, 1979, 3 448-454

[21] Tyystjärvi E., Vass I., Light emission as a probe of charge separation and recombination in the photosynthetic apparatus: Relation of prompt fluorescence to delayed light emission and thermoluminescence, In: Papageorgiou G.C., Govinjee (Eds.), Chlorophyll a fluorescence: A signature of photosynthesis, Springer, Dordrecht, 2004

[22] Krause G.H., Weis E., Chlorophyll fluorescence and photosynthesis: the basics, Annu Rev Plant Physiol Plant Mol Biol, 1991, 42, 313–349

[23] Samuilov V.D., Lagunova E.M., Dzyubinskaya E.V., Izyumov D.S., Kiselevsky D.B., Makarova Y.V., Involvement of chloroplasts in the programmed death of plant cells, Biochemistry (Moscow), 2002, 67, 627–634

[24] Teisseire H., Couderchet M., Vernet G., Phytotoxicity of diuron alone and in combination with copper or folpet on duckweed (Lemna minor), Environ Pollut, 1999, 106, 39–45

[25] Vavilin D.V., Polynov V.A., Matorin D.N., Venediktov P.S., Sublethal concentrations of copper stimulate photosystem II photoinhibition in Chlorella pyrenoidosa, J Plant Physiol, 1995, 146, 609–614

[26] Ouzounidou G., The use of photoacoustic spectroscopy in assessing leaf photosynthesis under copper stress: correlation of energy storage to photosytem II fluorescence parameters and redox change of P700, Plant Sci., 1996, 113, 229–237

[27] Briat J.-F., Metalion-activated oxidative stress and its control, In: Inze M., Van Montagu M. (Eds.), Oxidative stress in plants, Taylor & Francis, NewYork, 2002

[28] Krupa Z., Cadmium against higher plant photosynthesis: a variety of effects and where do they possibly come from?, Z Naturforsch, 1999, 54, 723–729

[29] Ciscato M., Vangronsveld J., Valcke R., Effects of heavy metals on the fast chlorophyll fluorescence induction kinetics of photosystem II: a comparative study, Z Naturforsch, 1999, 54, 735–739

[30] Houot L., Floutier M., Marteyn B., Michaut M., Picciocchi A., Legrain P., et al., Cadmium triggers an integrated reprogramming of the metabolism of Synechocystis PCC6803, under the control of the Slr1738 regulator, BMC Genomics, 2007, 8, 350

[31] Gomes-Junior R.A., Moldes C.A., Delite F.S., Pompeu G.B., Gratão P.L., Mazzafera P., et al., Antioxidant metabolism of coffee cell suspension cultures in response to cadmium, Chemosphere, 2006, 65, 1330–1337

[32] Kovac M., Ravnikar M., Sucrose and jasmonic acid interact in photosynthetic pigment metabolism and development of potato (Solanum tuberosum L. cv. Sante) grown in vitro, Plant Growth Regul, 1998, 24, 101–107

[33] ISO, Water quality - Determination of the toxic effect of water constituents and wastewater to duckweed (Lemnaminor) – Duckweed growth inhibition test, In: International Organization for Standardization, International Standard ISO, 20079

[34] Roháček K., Barták M., Technique of the modulated chlorophyll fluorescence: basic concepts, useful parameters, and some applications, Photosynthetica, 1999, 37, 339-363

[35] Bouvier F., Backhaus R.A., Camara B., Induction and control of chromoplast-specific carotenoid genes by oxidative stress, J Biol Chem, 1998, 273, 30651–3065

[36] Jursinic P.A., Delayed fluorescence: current concepts and status, In: Govindjee, Amesz J., Fork D.C. (Eds.), Light emission by plants and bacteria, Academic Press, Orlando, 1986

[37] Nedbal L., Soukupová J., Kaftan D., Whitmarsh J., Trtílek M., Kinetic imaging of chlorophyll fluorescence using modulated light, Photosynth Res, 2000, 66, 3–12

[38] Matous K., Benediktyova Z., Berger S., Roitsch T., Nedbal L., Case study of combinatorial imaging: what protocol and what chlorophyll fluorescence image to use when visualizing infection of Arabidopsis thaliana by Pseudomonas syringae?, Photosynth Res, 2006, 90, 243–253

[39] Zhang L., Xing D., Rapid determination of the damage to photosynthesis caused by salt and osmotic stresses using delayed fluorescence of chloroplasts, Photochem Photobiol Sci, 2008, 7, 352–360

[40] Gould P.D., Diaz P., Hogben C., Kusakina J., Salem R., Hartwell J., Hall A., Delayed fluorescence as a universal tool for the measurement of circadian rhythms in higher plants, Plant J, 2009, 58, 893–901